Available online at www.sciencedirect.com
ScienceDirect
Acta Materialia 57 (2009) 145–152
Acta MATERIALIA
www.elsevier.com/locate/actamat

Evidence of stress-induced hydrogen ordering in zirconium hydrides

A. Steuwer [a,b,*], J.R. Santisteban [c], M. Preuss [d], M.J. Peel [e], T. Buslaps [e], M. Harada [f]

[a] FaME38 at the ESRF-ILL, 6 rue J Horowitz, 38042 Grenoble, France
[b] ESS Scandinavia, University of Lund, Stora Algatan 4, 22350 Lund, Sweden
[c] Centro Atómico Bariloche, CNEA, San Carlos de Bariloche, Argentina
[d] University of Manchester, Grosvenor Street, Manchester M1 7HS, UK
[e] European Synchrotron Radiation Facility, 6 rue J Horowitz, 38042 Grenoble, France
[f] R&D Section, Chofu-Kita Plant, Kobe Special Tube Co, Shimonoseki 752-0953, Japan

Received 5 March 2008; received in revised form 9 July 2008; accepted 29 August 2008
Available online 11 October 2008

Abstract

The formation of hydrides in zirconium alloys significantly affects their mechanical properties and is considered to play a critical role in their failure mechanisms, yet relatively little is known about the micromechanical behavior of hydrides in the bulk. This paper presents the result of in situ uniaxial mechanical tensioning experiments on hydrided zircaloy-2 and zircaloy-4 specimens using energy-dispersive synchrotron X-ray diffraction, which suggests that a stress-induced transformation of the δ-hydride to γ-hydride via ordering of the hydrogen atoms occurs, akin to a Snoek-type relaxation. Subsequent annealing was found to reverse the ordering phenomenon.

Keywords: Hydrides; X-ray diffraction; Short-range ordering; Zircaloy

1. Introduction

Zirconium alloys are widely used in the nuclear industry as structural materials and as cladding for nuclear fuel in fuel assemblies. However, zirconium and its alloys have a considerable affinity for hydrogen, which readily diffuses into zirconium at high temperatures but has low solubility in the hexagonal α-phase. During operation in a boiling or pressurized water reactor, the cladding material will undergo aqueous corrosion. Some of the hydrogen which is produced during such corrosion is picked up by the zirconium cladding material and will lead to hydride precipitation once the solubility limit has been exceeded. As there is a temperature gradient between the inner surface (fuel = hot) and the outer surface (coolant = less hot) of the cladding, a hydride rim is typical after some operation time. It is well known that the presence and orientation of these hydrides adversely affect the mechanical properties of the material [1–3]. They can lead to embrittlement, delayed hydride cracking (DHC) and hydride blistering, all of which reduce the lifetime of the component and are cause for considerable environmental concern in the storage of spent fuel rods [1]. The widely accepted mechanism for DHC assumes that hydrogen diffuses along the stress gradients towards the tensile crack tip area where (re)precipitation of the brittle hydrides occurs, which at certain hydride size and stress intensity then encourages further propagation of the crack. Hydrogen can occupy interstitial tetrahedral and octahedral sites in hcp crystals, but for zirconium hydrides, the reported crystal structures from diffraction measurements indicate that mainly the tetrahedral sites are occupied. Two stable hydride phases, δ and ε, and one "metastable" hydride phase, γ, have been reported in the literature. The exact nature of the metastable phase remains controversial [4,5], and it is noteworthy that the reported stable δ-phase and metastable γ-phase essentially only differ in the degree of ordering of the

* Corresponding author. Address: FaME38 at the ESRF-ILL, 6 rue J Horowitz, 38042 Grenoble, France . Tel.: +33 476207945; fax: +33 476207943.
E-mail address: steuwer@ill.fr (A. Steuwer).

1359-6454/$34.00 © 2008 Acta Materialia Inc. Published by Elsevier Ltd. All rights reserved.
doi:10.1016/j.actamat.2008.08.061

hydrogen atoms on tetrahedral sites, which in turn affects the composition (see section 5). Yet, to the best of the authors' knowledge, no direct observation of a transition between the "ordered" and "unordered" states of the room temperature phases has been reported in the literature. Furthermore, the elusive metastable γ-phase is observed mostly after rapid quenching of the sample (e.g., >10 K min^{-1}) [3]. Improving understanding of the behavior and properties of these zirconium hydrides is therefore of significant importance. The hydride bands can be easily revealed by conventional laboratory-based imaging techniques, and it is well known that hydrides change orientation, depending on stresses [3]. However, these techniques are essentially surface techniques and provide very little information about the micromechanical properties of the hydrides, their crystallography and their relationship with the matrix [6] in the bulk, where the additional constraints are likely to change any transformation properties with respect to those occurring at the surface. This problem has been recognized, for example, in the study of martensitic transformation, to which the hydride transformation in zirconium alloys bears some resemblance [7,8].

Non-destructive characterization techniques such as neutron and high-energy synchrotron X-ray diffraction provide the capability to investigate phase-specific mechanical properties in bulk materials. For neutron diffraction, in order to overcome the large incoherent neutron scattering cross section of hydrogen, it is often replaced by its isotope deuterium [9]. Synchrotron X-rays, in contrast, are becoming increasingly popular for structural investigations of engineering materials, as third-generation synchrotron X-ray sources, such as the ESRF in Grenoble, France, yield an extremely high X-ray flux at energies high enough to penetrate metals. Unlike laboratory X-ray sources, this allows non-destructive investigations in bulk metallic components with a penetration depth of several millimeters, or even centimeters in light alloys at very high spatial resolution. Similarly, the large flux opens up the possibility of performing in situ mechanical testing with adequate time resolution, even in materials with a relatively high atomic number such as zirconium and on phases with a low volume fraction such as hydrides in zirconium.

The aim of this experiment was to undertake a uniaxial tensile test on hydrided zircaloy-2 and zircaloy-4 samples in order to study in situ the elastic response of different diffraction peaks (lattice planes) of both the matrix and the hydride phase under load and during plastic deformation. Such observations are expected to improve the understanding of the deformation and fracture mechanisms of hydrided zirconium alloys and provide valuable verification data for modeling approaches of failure mechanisms.

The experiment was performed using the high-energy beam line ID15A (ESRF) in energy-dispersive mode. The results revealed the anticipated response of the zirconium matrix, but showed surprisingly large d-spacing shifts of the hydride peaks incompatible with elasticity theory. The observed hydride peak shift can be explained by a stress-induced transformation of the hydride phase due to gradual ordering of the hydrogen atoms on the tetrahedral sites in the subset of grains most closely aligned with the loading direction, which is discussed here. Subsequent annealing resulted in a reverse hydride peak shift, which suggests reversal of the ordering process.

2. Brief review of the crystallography of hydrides

An overview of the zirconium hydrogen system can be found in the literature [9–12], and only the crystallographic information is summarized here for the sake of completeness. The dominant stable hydride phase in zircaloy-2 and zircaloy-4 at typical hydrogen concentrations of 300–600 ppm and room temperature is the non-stoichiometric δ-ZrH_2 phase, with a typical H/Zr ratio of ~1.66. This is a face-centered cubic (fcc) phase of the CaF_2 prototype ($Fm-3m$, $a = 4.768$ Å, Vol. $= 108.39$ Å^3) with four H atoms randomly occupying the eight available tetragonal $(0.25, 0.25, 0.25)$ sites. Additionally, a metastable tetragonal γ-phase (γ-$ZrH_{1.0}$) has been identified with an ordered tetragonal structure ($P\,4_2/n$, $a = 4.586$ Å, $c = 4.948$ Å, Vol. $= 104.06$ Å^3), where the hydrogen atoms occupy the tetrahedral sites on alternating (1 1 0) planes. The Zr atoms are found at the $(0.25, 0.25, 0.25)$ sites and H atoms at $(0, 0, 0)$ and $(0, 0, 0.5)$. Although inelastic neutron scattering experiments suggested a small orthorhombic distortion ($a \neq b$) and the $Cccm$ symmetry space group in 1994 [13], the distortion is relatively small, and the tetragonal $P\,4_2/n$ space group has been used as recently as 2003 [14]. The authors use the tetragonal space group for lack of sufficient instrumental resolution to resolve the difference and due to reasons explained further below.

The key difference between the reported γ-phase and the δ-phase is therefore the degree of ordering of the hydrogen atoms on the tetrahedral sites (and the associated change in composition), but no observation of any ordering transition at ambient temperatures has yet been reported in the literature.

The zirconium matrix is the hexagonal (hcp) α-phase ($P\,63/m\,m\,c$, $a = 3.2276$ Å and $c = 5.1516$ Å) with one Zr atom at $(0.333, 0.666, 0.25)$ where, for the sake of simplicity, the other alloying elements are ignored. A hydrogen-rich ε-phase (ZrH_2) also exists, which has a tetragonal space group of the ThH_2 prototype ($I\,4/m\,m\,m$ with $a = 4.9689$ Å, $c = 4.4497$ Å) and one Zr atom on $(0, 0, 0)$ and one H atom on $(0, 0.5, 0.25)$ [11], but which was not observed in the current investigation. As the main interest was in the relative movement of diffraction peaks, no specific attempts were made to calibrate the measured lattice spacing on an absolute scale, although the accuracy of reported values in terms of absolute values should be of the order of a few per cent of published lattice parameters.

3. Experimental

3.1. Sample preparation

The hydrided samples were prepared from zircaloy-2 and zircaloy-4 tubes. These alloys have a typical composition (in wt.%) of 1.3–1.6 Sn, 0.07–0.2 Fe, 0.05–0.16 Cr, 0.03–0.08 Ni and 0.13 other elements for zircaloy-2, and without the nickel and increased iron content for zircaloy-4. In both cases, the sample material was prepared from a tube 20 mm in outer diameter and 1.7 mm in wall thickness, which was cut along the tube axis parallel to the long tube direction and then pressed in order to obtain a flat plate. This was cold-rolled along the long direction to a thickness of 1.2 mm, which corresponds to a reduction in thickness of ~30%. Matchstick samples suitable for in situ tensioning were machined from this sheet with dimensions 3 mm wide (zircaloy-2) and 1.5 mm wide (zircaloy-4), 1.2 mm thick and 40 mm long. These specimens were then annealed at 580 °C for 2.5 h and hydrogen charged at 400 °C for 1 h in a hydrogen atmosphere. In this way, both alloys were charged to ~400 ppm by weight or (3.76 at.%). The distribution of the hydride phases in the starting material is shown in Fig. 1, which clearly reveals the dark bands of zirconium hydride.

The exact composition of the hydrides has not been established but, given the relatively low atomic per cent hydrogen charging, and that the hydrogen-rich ε-hydride phase was never identified experimentally, it can be assumed that the hydrides have a stoichiometric composition with an upper limit of $H/Zr \approx 1.7$.

3.2. The synchrotron X-ray diffraction set-up

The wiggler beam line [15] ID15A at the European Synchrotron Radiation Facility (ESRF) is capable of producing very high-energy X-rays in the region of 50–300 keV and can be operated in energy-dispersive mode. Unlike conventional laboratory X-ray diffraction, in this mode the scattering angle is kept fixed, and the diffracted beam is discriminated on the basis of photon energy. This is achieved with Ge solid-state detectors and a 8192-channel multi-channel analysers (MCA), where the channel number can be readily converted to photon energy, lattice spacing or other desired scales. In this case, two detectors were mounted at $5° = 2\theta$ (vertically and horizontally) with their scattering vectors virtually orthogonal, permitting the simultaneous measurement of the longitudinal and transverse strains in an appropriately oriented sample [16] (see Fig. 1). The incident slits were set to 0.1 mm opening gaps in the horizontal and vertical direction, and a pair of receiving slits to 0.1 mm horizontal gap for the horizontal detector and 0.1 mm vertical gap for the vertical detector, which were placed ~2 m from the sample. At such low Bragg angles, the instrumental resolution ($\sim\Delta\theta/\theta$) normally prevents the accurate determination of lattice strains in coarse-grained material, as the varying position of a large grain inside the gauge volume gives rise to changes in diffraction angles which, in turn, results in significant spurious measured strains. However, if the grain size of the material is sufficiently small with respect to the beam size, and hence gauge volume, a good powder average is achieved, and this effect essentially averages itself out [17].

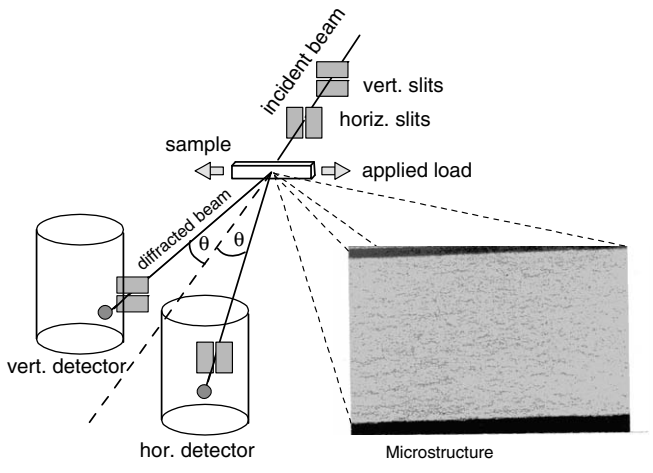

Fig. 1. A schematic of the experimental set-up showing the direction of loading, the two detectors, slits and additionally an optical micrograph of 415 ppm hydrided zircaloy-4 (50× magnification), revealing the dark bands of hydrides.

Tensile testing was performed on an electro-mechanical Instron tensile testing rig fitted with a 3 kN load cell. The direction of the applied stress was perpendicular to the incident beam and parallel to the horizontal direction. Testing was performed in displacement control at a strain rate of 0.1 mm min^{-1} for the zircaloy-2 specimen and 0.05 mm min^{-1} for the zircaloy-4 specimen with a gauge length of roughly 16 mm. Diffraction patterns were collected at 60 s (zircaloy-2) and 100 s (zircaloy-4) intervals in order to get sufficient intensity to be able to identify and distinguish the hydride peaks. The zircaloy-2 sample failed after 1698 s at a displacement of 2.84 mm, which is equivalent to an engineering strain ($\Delta L/L$) of ~17%, approximately in line with published values in the literature [2]. The zircaloy-4 sample failed at ~24.7%.

Fig. 2 shows the energy-dispersive diffraction pattern of the unloaded zircaloy-2 sample in the loading direction (longitudinal) and normal to it (transverse), revealing the matrix as well as the hydride diffraction peaks. As is common for zirconium cladding material [18], the matrix has a strong crystallographic texture, shown in Fig. 2 with, for example, the matrix peaks α-104, α-004 and α-103 being very strong in the transverse direction, where the α-103 peak partly overlaps with the δ-311 reflection, but being almost entirely absent in the longitudinal direction, incidentally permitting the analysis of the underlying hydride peak. The zircaloy-4 specimen showed a similar absence of certain reflections. A detailed discussion of the effects of texture as regards the micromechanics of hydrides is not feasible, owing to the weak nature of the hydride peaks

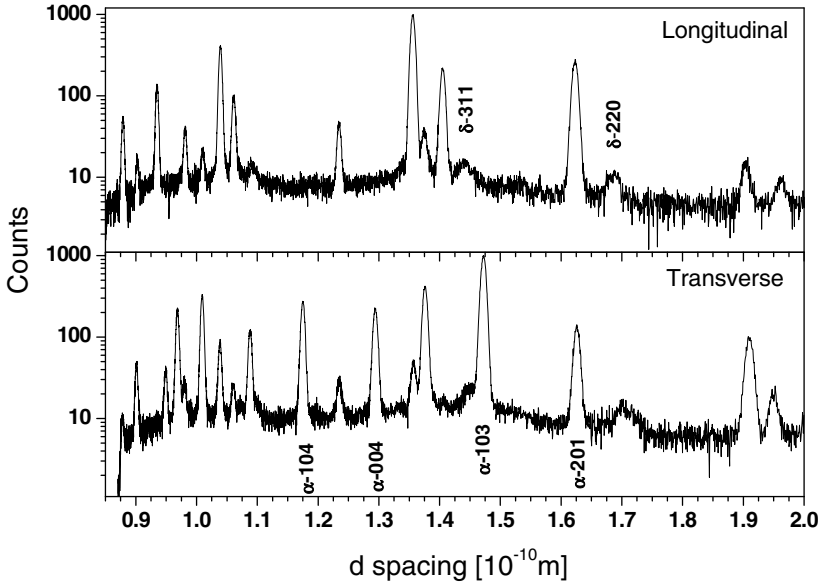

Fig. 2. The diffraction pattern in the longitudinal and transverse direction prior to loading plotted on a log scale to reveal the weak δ-hydride peaks. No other hydride phase has been identified within the achievable resolution. Note the strong crystallographic texture in the matrix.

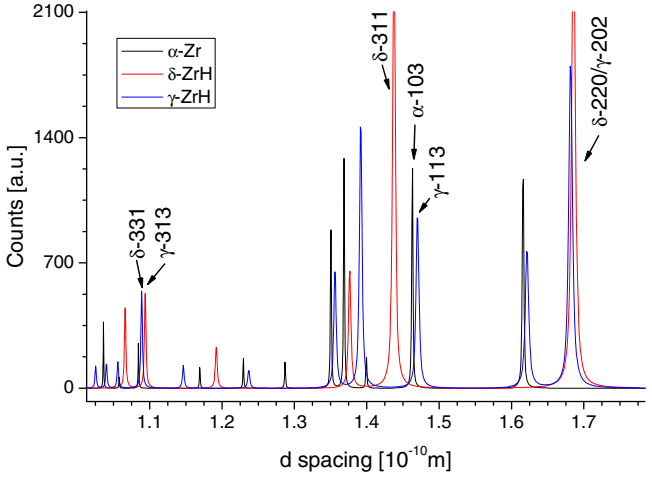

Fig. 3. The simulated diffraction patterns for α, δ, γ zirconium (hydride) and labeled for the three areas of matrix and hydride peaks shown in Fig. 5 (plotted with equal phase weighting).

and the fact that in the current setup we essentially only have two orientations with two detectors. Apart from the δ-phase, no other hydride phase has been identified initially to within the instrumental resolution.

Fig. 3 shows the calculated diffraction pattern for the α-Zr, δ-ZrH and γ-ZrH phases at equal weighting for comparison. Here, only the relevant hydride and matrix peaks, which are visible in the observed data in Fig. 5 and discussed in this paper, are labeled.

4. Results

Fig. 4 shows the macroscopic engineering stress–strain curve obtained from the INSTRON loading rig (left, continuous line) together with the lattice strain response of two representative matrix lattice planes, one for the longitudinal and one for the transverse direction (right scale), of the zircaloy-2 specimen. The diffraction peaks were fitted using pseudo-Voigtian profiles. Uncertainties are smaller than the symbol size in Fig. 4. Stresses are not inferred from the diffraction data for the sake of simplicity. The response of the matrix peaks, α-110 and α-103, in the longitudinal and transverse direction, respectively, is consistent with the macroscopic stress–strain curve, as expected for a ductile metal. In fact, the matrix response can be considered as a reference standard which supports the accuracy of the measured shift in the hydride peak. Considerable elastic/plastic anisotropy was observed for the different reflections in the transverse direction, as well as significant peak broadening, but any discussion of this effect is beyond the scope of this paper and will be presented elsewhere. To this end, two representative matrix reflections with relatively benign anisotropy were selected.

In contrast to the expected behavior of the matrix peaks, the observed δ-311 hydride peak for the zircaloy-2 specimen showed a very large lattice strain of the order of 22,500 με (= 2.25%) up to a macroscopic (applied) strain of ~4%. Beyond 4% macroscopic strain, which appears as a distinct discontinuity in the slope of the profile, the response follows more closely the change in matrix strain and increases by ~2000 με prior to failure of the specimen.

The considerable linear increase in lattice strain of nearly 2.25% and the observed profile in Fig. 4 are not consistent with the elastic–plastic behavior of most crystalline materials and suggest the occurrence of a transformation strain. Based on this observation, the experiment was then repeated on a zircaloy-4 specimen with a similar amount of hydrides but at slightly slower rates of displacement, in order to improve the counting statistics.

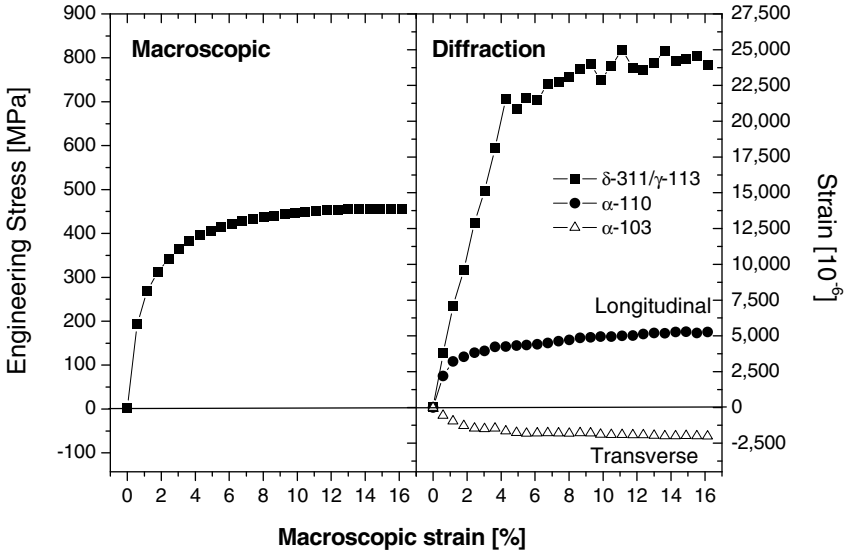

Fig. 4. The macroscopic stress–strain curve (left graph) compared with the lattice strain evolution measured using EDXRD (right graph) for the zircaloy-2 specimen. The evolution of the δ-311/γ-113 hydride peak shows an elastic (lattice) strain of ~2.25%. Error bars are of the order of the symbol size or less ($<10^{-4}$) and have been omitted.

The observed response of the hydride peak to the observed load could be reproduced in zircaloy-4, and the evolution of the δ-hydride, γ-hydride and the neighboring matrix peaks during the tensile test is more clearly illustrated in Fig. 5 as diffracted intensity (in *d*-spacing on the left and MCA channels on the right) against the macroscopic strain for the longitudinal direction. Fig. 5 shows three pairs of δ/γ-hydride peaks: the δ-220/γ-202; the δ-311/γ-113; and the δ-331/γ-313, see also Fig. 3. In all three cases, the δ-phase peaks display a significant linear shift towards larger *d*-spacing before gradually disappearing but, for the δ-311 case (Fig. 5b), this shift is the most pronounced. One must bear in mind that each reflection represents a different subset of grains with a different orientation of the main crystallographic axes *a* and *c* to the direction of the applied load. The magnitude of the linear strain observed for the δ-220/γ-202 pair as well as the δ-331/γ-313 pair is slightly less at ~1.16%.

5. Discussion

Comparing Fig. 5b with the theoretical pattern (Fig. 3), it appears as if the δ-311 hydride peak essentially "moves" towards the position of the γ-113 reflection, at which point there is a distinct change in the slope of the lattice strain response, also shown in Fig. 4 for the zircaloy-2 specimen. The predicted difference in lattice spacing between the δ-311 reflection (with a lattice spacing of $d_{\delta 311} = 1.43761$ Å) and the γ-113 reflection (with a lattice spacing of $d_{\gamma 113} = 1.47011$ Å) from Fig. 3 is ~2.26% and matches the measured strain of ~2.25%. For the zircaloy-4 specimen, the observed linear strain of the δ-311 reflection up to 4% macroscopic strain in Fig. 5b is slightly smaller at ~0.02 = 2% but still considerable.

The observed transformation can, however, be explained by the gradual, stress-induced ordering of the hydrogen atoms in a subset of the δ-hydrides whose crystallographic *a*-axis is most closely aligned with the loading direction. This ordering would be most pronounced in the δ-311/γ-113 reflection pair as, of the three hydride peaks observed in Fig. 5, the γ-113 is the closest to the [0 0 1] axis, which naturally orientates itself along the loading direction as the applied load elongates the cubic δ-phase in the direction of loading to form the tetragonal cell of the γ-phase. The hydrogen atoms, which before loading randomly occupied some of the available eight tetrahedral sites, are encouraged by the deformation to occupy those ordered tetrahedral sites which enable the elongation towards the tetragonal γ-phase in the direction of the applied load, namely those in the alternating (1 1 0) planes. It is in fact the pairing of hydrogen atoms on tetrahedral sites along the *c*-axis which causes the tetragonal distortion, akin to a Snoek-like relaxation [19,20] of the hydrogen atoms in the fcc δ-hydride. The observed continuous and uninterrupted peak shift in Fig. 5b suggests a homogeneous ordering process throughout the subset of hydrides which fulfill the diffraction condition in the loading direction. Any transformation based on the nucleation and growth of the γ-phase at the expense of the δ-phase would be readily distinguishable by synchrotron X-ray diffraction by the simultaneous appearance and disappearance of two separate peaks side by side, which was not observed. Furthermore, the linearity of the peak shift in Fig. 5b also suggests that the ordering is driven by and proportional to the applied stress, and that any threshold stress to initiate the ordering process is very low. The threshold energy would be equivalent to that required to initiate the hydrogen movement between tetrahedral and octahedral sites, of

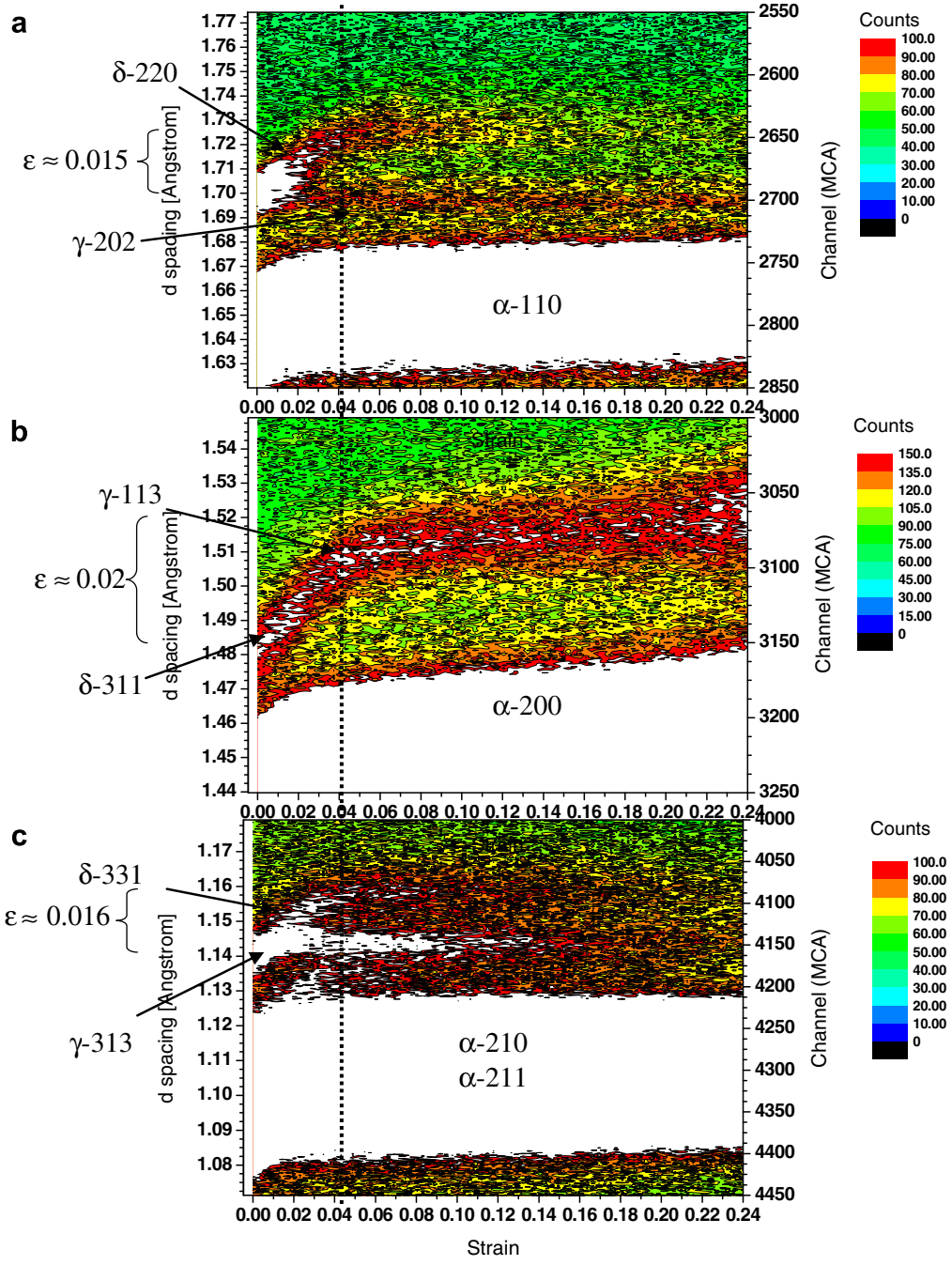

Fig. 5. Comparison of the evolution of the hydride peaks in the zircaloy-4 sample under applied load as contour plots of raw channel (corresponding to *d*-spacing) and macroscopic strain. The intensity of the matrix (α) peaks exceeds the current scale and is rendered white: (a) evolution of the δ-220/γ-202 peak; (b) evolution of the δ-311/γ-113 peaks; (c) evolution of the δ-331/γ-313 peak. In all three cases, the peak behaviour changes at a macroscopic strain of ≈4%.

the order of 0.5 eV [21,22]. Furthermore, the immediate response of the observed diffraction peak indicates that the diffusion and ordering of the hydrogen atoms occurs on timescales equal to or faster than that of the rate of displacement in this tensile test.

Furthermore, the ordering transition implies that a small amount of excess hydrogen (the γ-phase has a nominal stoichiometric ratio H/Zr = 1) is expelled from the subset of hydrides which are favorably aligned for observation by diffraction into the surrounding matrix, aided by the high mobility of hydrogen in zirconium, which equally facilitates the ordering process, as already noticed and discussed by Cassidy and Wayman [7].

As indicated in Fig. 5 by the vertical dashed line across a, b and c, the transformation appears to be complete at 4% macroscopic strain. This value is equal to the volume change of the slightly larger δ-ZrH ($V = 108.39$ Å^3) phase compared with γ-ZrH ($V = 104.06$ Å^3), and furthermore

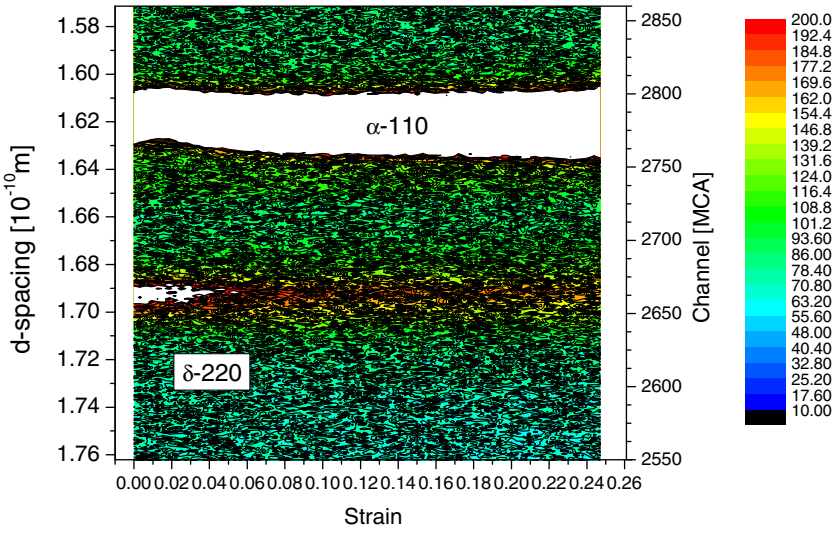

Fig. 6. The δ-220 peak in the transverse direction does not display any significant movement during tensile loading.

agrees with the observed and calculated shape strain for the δ-to-γ transformation using the phenomenological theory of martensitic transformation [7]. In the present case, the observed transformation strain (resembling a Bain strain) would then be akin to the formation of a single Bain correspondence variant [23] and further corroborate the resemblance to stress-induced martensitic transformations. The observed behavior suggests that the ordering process occurs in response to the loading but that the γ-phase only begins to share the applied load once the ordering process is complete at 4% applied strain, which explains the discontinuity in the slope of the response of the hydride peak of Fig. 5. The increasing ordering of hydrogen atoms causes the gradual disappearance of the δ-hydride peaks in Fig. 5a and c. As these peaks are less well aligned to the loading direction, the ordering is only partially achieved. In fact, given the possible orientation of the alternating (1 1 0) planes in the unit cell, there are several ways in which partial ordering would introduce distortions to the cubic or tetragonal cell of the hydride which may account for the *Cccm* distortion observed by Kolesnikov et al. [13].

Fig. 6 shows the evolution of the δ-220 hydride peak in the transverse direction during loading. Unlike in the loading direction, and the nearby matrix peak, no significant *d*-spacing shift is observed, confirming the preferential ordering along the direction of loading. The other hydride peaks of Fig. 5 b and c are not shown, as they are obscured by matrix peaks in this direction. In the current set-up (see Fig. 1), only two (virtually orthogonal) directions – longitudinal and transverse – were measured but, using a set-up involving a 2D detector, it should be possible to observe the gradual ordering with increasing alignment with the loading direction.

As the increasing ordering represents lower entropy, it should be possible to reverse the ordering process by annealing, during which the hydrogen atoms redistribute randomly amongst the tetrahedral sites, and residual stresses are relaxed. Fig. 7 compares the same part of the diffraction pattern as Fig. 2 in the longitudinal direction before and at maximum applied strain, as well as after a

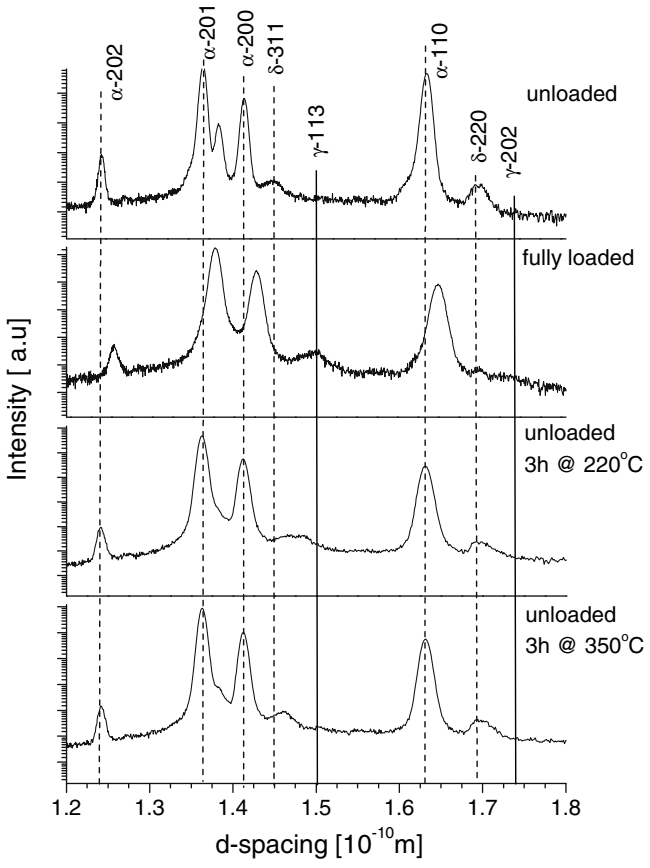

Fig. 7. The effect of loading and subsequent annealing on the diffraction pattern. After 3 h at 220 °C, a broad mixed peak of δ and γ is visible, whereas after a further 3 h at 320 °C, the γ-hydride peak has almost vanished. However, the δ-311 peak does not fully recover its original position.

two-step annealing process, first 3 h at 220 °C and then 3 h at 350 °C. Upon straining, the δ-311 peaks clearly moves more than the matrix peaks to the location of the γ-113 peak, as discussed earlier. After the first step of annealing at 220 °C, the γ-113 peak has partly retransformed to the δ-311 peak, and two neighboring hydride peaks are visible. After the second annealing step at 350 °C, the γ-113 has almost completely transformed back into the δ-311, although it does not return fully to its original position. This is either the incomplete reverse transformation or due to a difference in stoichiometric composition between the initial and final δ-phase, as the former needed to expel the excess hydrogen in order to achieve a lower composition that allowed the formation of the γ-hydride phase.

It is furthermore noteworthy that, in the γ-hydride, the movement of two hydrogen atoms per unit cell from the tetrahedral sites on the (1 1 0) plane onto the tetrahedral sites of the (0 1 1) plane will cause a 90° rotation of the *c*-axis of the tetragonal cell. The Snoek-type movement of hydrogen following applied (or residual) stresses may well be the basic mechanism that lies behind the observed reorientation of hydrides due to applied stresses. The observed ordering is, to the best of the authors' knowledge, the first time that a Snoek-like relaxation has been observed directly by diffraction, and in a precipitate rather than in the bulk matrix.

The ordering process as a function of applied stress also serves to illuminate the existing controversy on the stability and kinetics of the metastable γ-phase [4]. The presence of macroscopic to inter- or intragranular residual stresses due to the thermo-mechanical history, in particular plastic deformation, of the material may have induced some ordering, leading to varying amounts of γ-hydride with strong preferred orientation along the tensile stress regions with complex coupling to subsequent annealing/stress–relaxation behavior and other micromechanical factors and texture. Whether the γ-phase is observed depends on the orientation of the stress field, as shown in this experiment, and where the diffraction measurements are being undertaken. Hence, the γ-phase is frequently observed with neutron diffraction, which has strong penetration capabilities [14] but less so with laboratory X-ray systems, where measurements are only carried out on the surface which, by definition, is stress free in the normal direction [4].

6. Conclusions

The results from in situ tensile testing experiments on hydrided zircaloy specimens showed unusually large strains in the hydride phase in the direction of loading. These strains are incompatible with basic elasticity theory but can be explained by a strain-induced hydrogen ordering phenomenon, which causes a transformation of the δ-hydride to a γ-hydride in the subset of grains which are suitably aligned with the loading direction. The hydrogen ordering occurs on the tetrahedral sites of the matrix, and therefore bears some resemblance to a Snoek-type relaxation. It was observed at relatively slow strain rates and is completed at ~4% applied strain, which coincides with the ratio between the unit cells of the two hydride phases, as well as the observed shape strain in a martensitic type δ/γ transformation. The effect of strain rate, texture and levels of hydridation on this transformation remains to be investigated. The transformation was found to be reversible by annealing the specimen.

The experiment also highlights that, for the first time, it has been possible to measure the lattice strain evolution during in situ loading of a metallic material using energy-dispersive synchrotron X-ray radiation. The data allowed the investigation of the matrix as well as the minority hydride phase.

Acknowledgements

The authors acknowledge access to synchrotron X-rays at the ESRF, and Dr. J.E. Daniels (ESRF), Profs. P.J. Withers and T. Mori (Manchester University) for many useful and illuminating discussions.

References

[1] IAEA, 2004, IAEA-TECDOC-1410: Vienna.
[2] Chu HC, Wu SK, Chien KF, Kuo RC. J Nucl Mater 2007;362:93.
[3] Ells CE. J Nucl Mater 1968;28:129.
[4] Lanzani L, Ruch M. J Nucl Mater 2004;324:165.
[5] Nath B, Lorimer GW, Ridley N. J Nucl Mater 1973/1974;49:262.
[6] Une K, Nogita K, Ishimoto S, Ogata K. J Nucl Sci Technol 2004;41:731.
[7] Cassidy MP, Wayman CM. Metall Trans A Phys Metall Mater Sci 1980;11:47.
[8] Cassidy MP, Wayman CM. Metall Trans A Phys Metall Mater Sci 1980;11:57.
[9] Sidhu SS, Sataya Murthy NS, Campos FP, Zauberis DD. Adv Chem Ser 1963;39:87.
[10] Zuzek E, Abriata JP, San-Martin A, Manchester FD. Bull Alloy Phase Diagrams 1990;11:385.
[11] Zuzek E, Abriata JP, San-Martin A, Manchester FD. In: Manchester FD, editor. Phase diagrams of binary hydrogen alloys. Materials Park, OH: ASM International; 2000. p. 309.
[12] Beck RL. Trans Am Soc Met 1962;55:542.
[13] Kolesnikov AI, Balagurov AM, Bashkin IO, Belushkin AV, Ponyatovsky EG, Prager M. J Phys Condens Matter 1994;6:8977.
[14] Root JH, Small WM, Khatamian D, Woo OT. Acta Mater 2003;51:2041.
[15] Tschentscher T, Suortti P. J Synchrotron Radiat 1998;5:286.
[16] Steuwer A, Santisteban JR, Turski M, Withers PJ, Buslaps T. J Appl Crystallogr 2004;37:883.
[17] Steuwer A, Peel M, Buslaps T. In: European conference on residual stresses vii; 2006. p. 267.
[18] Gloaguen D, Francois M, Guillen R, Royer J. Acta Mater 2002;50:871.
[19] Teus SM, Shyvanyuk VN, Gavriljuk VG. Acta Mater 2006;54:3773.
[20] Sinning HR. Mater Sci Eng A Struct Mater Properties Microstruct Process 2006;442:99.
[21] Wipf H, Kappesser B, Werner R. J Alloys Compd 2000;310:190.
[22] Sholl DS. J Alloys Compd 2007;446–447:462.
[23] Mori T, Oliver EC, Daymond MR, Withers P. Mater Sci Eng A Struct Mater Properties Microstruct Process 2004;378:479.